

Self-organized criticality in nonconservative mean-field sandpiles

Dranreb Earl Juanico

Rm 3111 Complex Systems Theory Group, National Institute of Physics,
 University of the Philippines, Diliman, Quezon City, Philippines 1101
 e-mail: djuanico@gmail.com

Received: date / Revised version: date

Abstract. A mean-field sandpile model that exhibits self-organized criticality (SOC) despite violation of the grain-transfer conservation law during avalanches is proposed. The sandpile consists of N agents and possesses background activity with intensity $\eta \in [0, 1]$. Background activity is characterized by transitions between two stable agent states. Analysis employing theories of branching processes and fixed points reveals a transition from sub-critical to SOC phase that is determined by ηN . The model is used to explain the school size distribution of free-swimming tuna as a result of population depletion.

PACS. 05.65.+b Self-organized systems – 05.70.Fh Phase transitions: general studies – 89.75.Da Systems obeying scaling laws

1 Introduction

Prototypical SOC sandpile models have attracted several researchers due to their inherent simplicity yet non-trivial behavior. Dynamical mean-field theory has been proven to offer the most effective elucidation of how SOC works [1]. One of the key ingredients found to bring about SOC in sandpiles is grain-transfer conservation. Tsuchiya and Katori offered rigorous proof that violation of the conservation law frustrates the criticality of Abelian sandpiles [2]. A mean-field treatment of the Manna sandpile known as the self-organized branching process (SOBP) has been proposed, further demonstrating that nonconservation disrupts criticality [3]. Breaking of SOC due to nonconservation has also been later demonstrated numerically and analytically in the Olami-Feder-Christensen earthquake model [4]. The forest-fire model (FFM), which does not have conservation laws, was also proposed as a model for SOC [5]. However, it was ultimately proven, via analysis of Lyapunov exponents [6] and later by means of renormalization group approach [7], that FFM does not exhibit SOC.

Signatures of scale invariance and criticality in biology, ecology, and a wide range of other animate complex systems have been linked to the principles behind power-law generating SOC models such as the sandpile model [8]. Practically, biological systems are not expected to be conservative either because they are constantly interacting with the environment and are far from equilibrium. These systems are therefore not supposed to display SOC.

Here, I propose a mean-field sandpile model that displays criticality despite violation of grain-transfer conservation. This model takes off from the conceptual difficulty with typical sandpile models in defining fluctuations be-

tween stable states because passive sites only switch states when an avalanche crosses them or when a grain is sprinkled on them. Thus, sites in this model are turned into *active agents*. Demonstrating criticality in self-organizing systems that are nonconservative enhances the synthetical capacity of SOC theory in the arena of biocomplexity.

Section 2 describes the nonconservative model. Section 3 presents and discusses the results of analysis and simulations of the model. Section 4 elaborates salient assumptions and possible areas for further analysis and extension. Lastly, Section 5 summarizes and concludes the paper.

2 Model

2.1 Framework

Inspired by biocomplexity, a sand grain assumes the role of a stimulus—for instance an environmental trigger—that is stored, integrated, and transferred from one agent to another. The build-up of stored stimuli induces agent response, which activates the transfer of stimulus through neighboring agents. Stimulus propagation corresponds to avalanches.

In accordance with Manna sandpile rules and studies of excitable media [9], each agent in the system may be in any three states {refractory, quiescent, excited} mapped to $\{z\} = \{0, 1, 2\}$, as follows:

- quiescent $\mapsto z = 1$
- excited $\mapsto z = 2$
- refractory $\mapsto z = 0$

By storage and integration of stimulus, refractory agents may turn quiescent and quiescent agents may become excited. If threshold $z_{\text{th}} = 1$, then an excited agent's stimulus level $z > z_{\text{th}}$, so that it fires a response in order to relax back to the stable states $z = 0, 1$. When this happens, an avalanche ensues. "Avalanche" is here interpreted as *clustering* in the sense that the agents excited during an avalanche are all "behaviorally matched" to the initial agent that triggers the avalanche.

This model differs from typical sandpile models because it allows for the possibility that, apart from excitations triggered along the path of the avalanche, a refractory agent can spontaneously become quiescent and vice versa, albeit at a much slower pace than the avalanche itself. This independent but slow process is what is referred hereafter as *background activity*.

The system is a population of $N = 2^{n+1} - 1$ excitable agents, where n corresponds to the maximum number of generations of excitation allowed during a single avalanche, so that n is a boundary condition. The model has no explicit dependence on any spatial lattice configurations, which makes analysis straightforward due to the absence of nearest-neighbor correlations and is a more accurate representation of socially interacting systems made up of entities that are constantly in motion such as animal groups. The mean-field nature of the model also does not require a physical boundary. Fish schools, for instance, traverse a seemingly limitless oceanic space.

2.2 Mean-Field Transition Rules

The population dynamically reconfigures the landscape of agent states when there is no avalanche. A quiescent agent turns refractory with probability λ , whereas a refractory agent turns quiescent with probability η . These transitions between refractory and quiescent states (stable agent states) is the background activity.

The time-dependent density $q(t)$ of quiescent agents also corresponds to the probability that an external stimulus injected at time t into a randomly selected agent initiates excitation, because only quiescent agents can become excited at any given time. If at time t an excited agent indeed emerges, time is frozen and avalanche ensues. Freezing time follows from the assumption that background activity takes place much slower than an avalanche—known as "timescale separation," which is a typical assumption in sandpile models [1].

During an avalanche, an excited agent stimulates at most two other agents. With probability α the excited agent turns refractory by transferring 2 units of stimuli to two randomly chosen neighbors. With probability β the excited agent turns quiescent by dissipating only 1 unit of stimulus to one random neighbor. Incorporating a probability $\epsilon = 1 - \alpha - \beta$ that an excited agent turns refractory by inwardly absorbing 2 units of stimuli without subsequently stimulating other agents, the transfer rule becomes nonconservative. Conservation law is therefore violated for $\epsilon > 0$.

Table 1. Mean-field transition rules of the nonconservative branching model with corresponding transition probabilities. The central digits for the avalanche rules correspond to the excited agent and the flanking digits are the two random neighbors, in no particular order. The sum of transition probabilities for the avalanche and nonconservative rules is q , which is, self-consistently, the probability that the avalanche had initiated.

Process	Rule	Transition probability
Background	$1 \rightarrow 0$	λq
	$0 \rightarrow 1$	$\eta(1 - q)$
Avalanche (branching process)	$121 \rightarrow 202$	αq^3
	$021 \rightarrow 102$	$2\alpha q^2(1 - q)$
	$020 \rightarrow 101$	$\alpha q(1 - q)^2$
	$121 \rightarrow 112$	βq^3
	$021 \rightarrow 012$	$2\beta q^2(1 - q)$
	$020 \rightarrow 011$	$\beta q(1 - q)^2$
Nonconservation	$2 \rightarrow 0$	$\epsilon q = (1 - \alpha - \beta)q$

The nonconservative transfer rule repeats until all excited agents are depleted, after which the frozen time takes off again and the population builds up for the next avalanche. There is a limit n to the number of generations of transfers during an avalanche. At the n -th generation, any remaining excited agents mandatorily absorbs stimuli without further stimulation of other agents. All the aforementioned processes are summarized in table 1.

2.3 Dynamics and Branching Process

Given the transition rules, the density q , assumed to be a continuous dynamical variable, satisfies the stochastic dynamical equation

$$\frac{dq}{dt} = (1 - q)\eta - q\lambda + \mathcal{A}(q; \alpha, \beta) + \xi(t)/N. \quad (1)$$

The noise term ξ/N arises from the stochastic transition rules, accounting for fluctuations around mean values assumed to hold in the mean-field calculations. It appropriately vanishes in the large- N limit. The term $\mathcal{A}(q; \alpha, \beta)$ represents the change in $q(t)$ due to redistribution of stimulus by an avalanche at time t . Treating an avalanche as a branching process, and following closely the analysis in [3], $\mathcal{A}(q; \alpha, \beta)$ satisfies

$$N\mathcal{A} = 1 - \sigma^n - \frac{\epsilon q}{1 - (1 - \epsilon)q} \left[1 + \frac{1 - \sigma^{n+1}}{1 - \sigma} - 2\sigma^n \right], \quad (2)$$

where σ is the branching parameter derived from the following definition

$$\sigma = \sum_k k\pi_k, \quad (3)$$

wherein from table 1, the branching probability π_k that an excited agent subsequently stimulates k other agents is

$$\pi_k = \alpha q \delta_{k,2} + \beta q \delta_{k,1} + [1 - (1 - \epsilon)q] \delta_{k,0}, \quad (4)$$

with $\delta_{i,j}$ being the Kronecker delta. The first and second terms in eq. (4) are the sum of transition probabilities of the first three avalanche rules and of the last three

avalanche rules listed in table 1, respectively. The last term is the total probability coming from the nonconservation rule and the case wherein a subsequently stimulated agent is refractory, which both result to $k = 0$. Substitution of eq. (4) into eq. (3) gives

$$\sigma = (2\alpha + \beta)q, \quad (5)$$

which depends on α and β , and is proportional to density q . In this model it is assumed that α and β remain fixed throughout so that the only dynamic variable is q . Consequently,

$$\frac{d\sigma}{dt} = (2\alpha + \beta) \frac{dq}{dt}. \quad (6)$$

A branching process is sub-critical when $\sigma < 1$, and consequently avalanches have sizes always smaller than a finite cutoff size. On the other hand, a branching process is supra-critical when $\sigma > 1$, and consequently avalanches with sizes as large as the system itself are formed almost with certainty. Hence, $\sigma = 1$ is a critical value that results to a critical branching process [10]. The avalanche size distribution emerging from a critical branching process is expected to be power law. Since σ only varies when q changes, the q determines whether the branching process is sub-critical, critical, or supra-critical.

To keep the model minimal, the number of parameters in eq. (1) is reduced by introducing the relation

$$\begin{aligned} \frac{\lambda}{\eta} &= \sigma/q - 1 \\ &= 2\alpha + \beta - 1, \end{aligned} \quad (7)$$

which effectively couples the background activity to the avalanche (branching process). Eq. (7) is a phenomenological assumption which essentially guarantees that $q(t)$ in the steady state approaches a value that makes $\sigma = 1$. This is an indication that the model self-organizes to its critical state. In order to analytically prove that the model indeed exhibits SOC, the critical state must be an attractive fixed point in phase space [7]. The phase portrait is simply a plot of $\dot{q} := dq/dt$ versus q . Since $\sigma \propto q$, then the phase portrait can equivalently be visualized by plotting $\dot{\sigma} := d\sigma/dt$, defined in eq. (6), versus σ .

2.4 Avalanche Size Distribution

An avalanche resulting from the rules of the model is illustrated as a branching tree in figure 1. The initial excited agent is the topmost node, giving rise to two subsequently excited nodes with probability αq . One of these excited nodes in turn generates one excited node with probability βq , while the other generates two excited nodes with probability αq . One of such excited nodes do not generate a subsequently excited node with probability ϵq due to nonconservation. Setting $n = 3$, all excited nodes at three levels below the topmost node do not further generate excited nodes. In the example shown, the avalanche size $s = 9$.

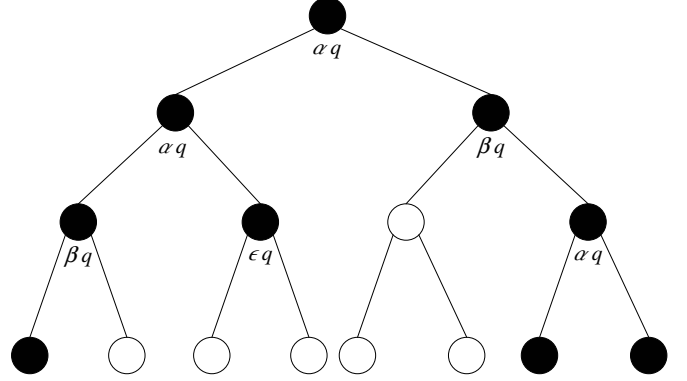


Fig. 1. Avalanche for $n = 3$ shown as a branching tree. Shaded circles correspond to excited agents. The avalanche size $s = 9$ corresponds to the total number of shaded circles.

The branching probability π_k defined in eq. (4) essentially describes the likelihood that an excited agent subsequently generates $k \in \{0, 1, 2\}$ excited agents in the succeeding generation. Using π_k the avalanche size distribution $P(s)$ is calculated via a generating functional formalism. A generating function $\mathfrak{F}_m(\omega)$ for $P(s)$ after m generations is defined as

$$\mathfrak{F}_m(\omega) = \sum_{s=1}^{\infty} P(s) \omega^s. \quad (8)$$

Incidentally, \mathfrak{F}_m is also the m -th iterate of the generating function $\mathfrak{F}_1 := \mathfrak{F}$, defined as

$$\mathfrak{F}(\omega) = \sum_{s=1}^{\infty} \pi_{s-1} \omega^s = \omega \sum_{s=1}^{\infty} \pi_{s-1} \omega^{s-1}. \quad (9)$$

Also by definition, $\mathfrak{F}_{m+1} = \mathfrak{F}(\mathfrak{F}_m)$, such that from eq. (9) one obtains

$$\mathfrak{F}_{m+1}(\omega) = \omega \sum_{s=1}^{\infty} \pi_{s-1} [\mathfrak{F}_m(\omega)]^{s-1},$$

which simplifies to

$$\mathfrak{F}_{m+1}(\omega) = \omega \{ \alpha q \mathfrak{F}_m^2 + \beta q \mathfrak{F}_m + [1 - (1 - \epsilon)q] \}, \quad (10)$$

following from the definition of π_k in eq. (4). For large enough m , the theory of branching processes asserts a self-consistency relation wherein $\mathfrak{F}_{m+1} \simeq \mathfrak{F}_m$, so that solving for \mathfrak{F}_m in eq. (10) yields

$$\mathfrak{F}_m(\omega) = \frac{1 - b\omega - \sqrt{1 - 2b\omega + a\omega^2}}{2\alpha q\omega}, \quad (11)$$

where $a = \beta^2 q^2 - 4\alpha q[1 - (1 - \epsilon)q]$, and $b = \beta q$. Binomial expansion of eq. (11) around its singularity $\omega = 0$, one obtains a power series similar to eq. (8). The coefficients of this expansion correspond to $P(s)$ from eq. (8). In a more compact form the solution can be expressed as a recurrence relation

$$P(s) = \frac{1}{s+1} [(2s-1)bP(s-1) - (s-2)aP(s-2)]. \quad (12)$$

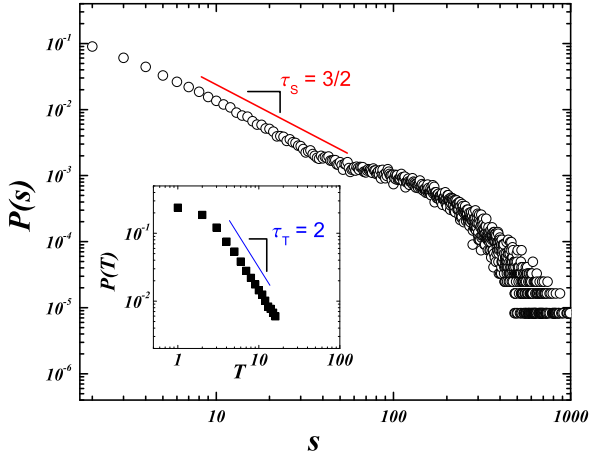


Fig. 2. Avalanche size distribution of a nonconservative system with $\epsilon = 0.2$ and $\eta N \approx 8192$. A power-law with exponent $\tau_s = 3/2$ is drawn as guide to the eye. The exponential fat tail is an artifact of the finiteness of the system. The inset graph is the distribution of avalanche lifetimes, which is the number of excitation generations before the avalanche dies out. A power law with exponent $\tau_T = 2$ is drawn as guide.

Eq. (12) may be shown, by graphical inspection, to have the asymptotic behavior $P(s) \sim s^{-3/2}$ for $s \gg 1$ if $a = 2b - 1$; a condition that can equivalently be expressed as

$$\begin{aligned} Q(q) &= a + 2b - 1 \\ &= \beta^2 q^2 - 4\alpha q[1 - (1 - \epsilon)q] - 2\beta q + 1 \\ &= 0. \end{aligned} \quad (13)$$

Numerical simulation of the model also confirms the asymptotic behavior of eq. (12), as shown in figure 2, for degree of nonconservation $\epsilon = 0.2$ and $\eta N \approx 8192$.

The function $Q(q)$ is parabolic in terms of q and has a unique root at $q_c = (2\alpha + \beta)^{-1}$, which makes $\sigma = 1$. Hence, eq. (13) is a criticality condition. Furthermore, since $\sigma \propto q$, then $Q(q)$ can alternatively be expressed as $Q(\sigma)$ which has a root at $\sigma = 1$.

3 Results and Discussion

The stationary behavior of the model is examined using a well-established geometrical theory of fixed points [11]. Nonlinear differential equations such as eq. (6) may be analyzed graphically in terms of vector fields. In this framework $\dot{\sigma}$ is interpreted as a “velocity vector” at each possible σ value. Plotting $\dot{\sigma}$ versus σ is the phase portrait of the model. The fixed point σ^* is the value of σ at which $\dot{\sigma} = 0$. The trajectory of the vector around the neighborhood of this fixed point is directed to the right where $\dot{\sigma} > 0$, and to the left where $\dot{\sigma} < 0$. This means that if $\dot{\sigma}$ is increasing around the neighborhood of σ^* , then the fixed point is repulsive. On the other hand, if $\dot{\sigma}$ is decreasing, then the

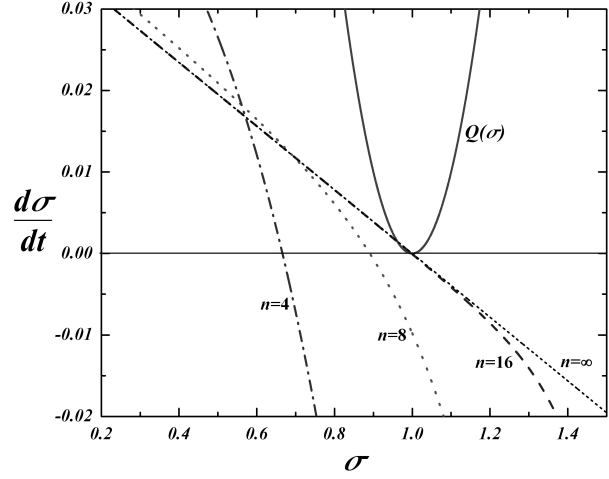


Fig. 3. Phase portrait showing $\dot{\sigma}$ versus σ , of a nonconservative system with $\epsilon = 0.25$ and $\eta = 0.03125$ for different n : 4 (chain curve), 8 (dotted curve), 16 (dashed curve), and ∞ (broken line). The root of $\dot{\sigma}$ corresponds to the fixed point value σ^* of the branching parameter. The solid parabolic curve is the function $Q(\sigma)$ with root at $\sigma = 1$. For $n \geq 16$, $\sigma^* = 1$, which indicates that the nonconservative system evolves towards its critical state via self-organization.

fixed point is attractive. Linearization of eq. (6) actually yields

$$\lim_{\sigma \rightarrow \sigma^*} \frac{\partial}{\partial \sigma} \frac{d\sigma}{dt} < 0.$$

Shown in figure 3 are the phase portraits of the model for different n , which are monotonically decreasing. Thus, the fixed points of eq. (6) are indeed dynamically attractive. Therefore, apart from fluctuations, the model spontaneously approaches the state defined by its fixed point—the very idea of self-organization.

Also illustrated in figure 3 is the function $Q(\sigma)$ with a root at $\sigma = 1$. For $n = 4$ and $n = 8$, obviously $\sigma^* < 1$, implying that the system self-organizes towards a sub-critical state. However, from $n = 16$ up to $n \rightarrow \infty$, $|\sigma^* - 1| \ll 1$. A nonconservative system achieves criticality even if its size is finite. The rapid approach of σ^* towards 1 from $n = 8$ to $n = 16$ and the decelerating change in σ^* from $n = 16$ to $n \rightarrow \infty$ indicates a phase transition.

Indeed, as shown in figure 4, a phase transition of the model exists. The data points are derived from numerical fixed-point analysis of eq. (1), assuming that the noise term ξ/N is very small to be significant. For a wide range of parameter values: $\epsilon \in (0, 1/2)$ and $\eta \in (0, 1]$, a transition surfaces out from the relation between ηN and $(q^* - 1/2)/(q_c - 1/2)$. The resultant plot is fitted by a logistic curve

$$\frac{q^* - 1/2}{q_c - 1/2} = 1 - \left[1 + \left(\frac{\eta N}{\theta} \right)^\gamma \right]^{-1}, \quad (14)$$

where $\theta = 9.31 \pm 0.27$ and $\gamma = 0.68 \pm 0.01$ (goodness of fit: $\chi^2/\text{DoF} = 4 \times 10^{-5}$, $R^2 = 0.99986$, no weighting). Eq. (14) suitably describes two limiting cases. The first one is $\eta \rightarrow 0$, which results to $q^* \rightarrow 1/2$. This limiting

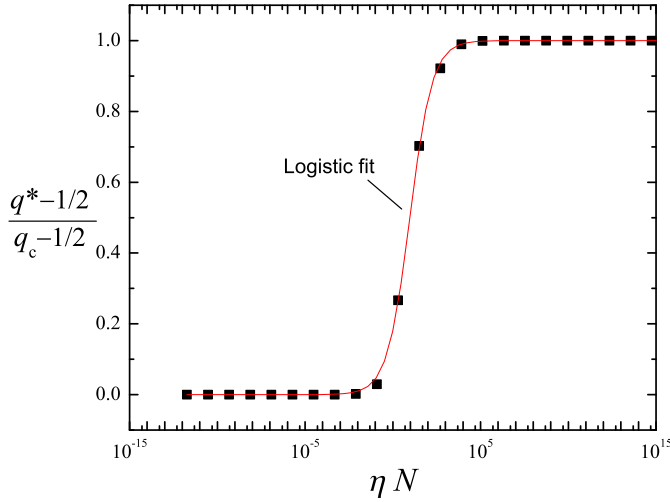


Fig. 4. Phase transition in the nonconservative branching model. Data points result from numerical analysis of the fixed points q^* of Equation 1 neglecting fluctuations ξ/N , for various $\epsilon \in (0, 0.5)$, $\eta \in (0, 1]$, and system size N . The curve is a logistic fit of the form $y(x) = 1 - [1 + (x/\theta)^\gamma]^{-1}$ where $y = (q^* - 1/2)/(q_c - 1/2)$ and $x = \eta N$.

case is equivalent to having no background activity, as in the SOBP model by Lauritsen, Zapperi & Stanley [3]. They have similarly found that the steady-state (fixed-point) value is $q^* = 1/2$, irrespective of any degree of nonconservation ϵ . Consequently, their sandpile model is always sub-critical whenever $\epsilon > 0$.

The second limiting case is $nN \gg \theta$, which leads to $q^* \rightarrow q_c$. At this limit, the nonconservative system is always critical. A closer look at figure 4 reveals that the data points lie considerably close to 1 starting at $\eta N \sim 10^4$. This means that if the population is very large, say $N = 10^9$, then for a wide range of $\eta \in (10^{-5}, 1]$ the nonconservative system achieves SOC. Simulation of the model for various degrees of nonconservation ϵ yields an avalanche size distribution of the form plotted in figure 2.

In the context of ecological systems, large N may easily be satisfied by clumps of microorganisms such as cellular aggregates in culture [12]. However, in macroscopic systems such as animal groups, this may not be the case because of several ecological factors, such as the presence of predators and destruction of habitats, which curtail the proliferation of a certain species. A good example is a population of tuna fishes studied by Bonabeau et al. [13]. The school size distribution $P(s)$ found from this study is plotted in fig. 5, fitted by the nonconservative model with $\epsilon = 0.15$ and $\eta N = 409.5$. This ηN value maps to a sub-critical phase on the phase diagram shown in figure 4, explaining the prominent exponential tail in $P(s)$. Also shown is a curve from an equivalent SOBP model [3], exhibiting less agreement with the data.

A school size distribution having an exponential tail implies that schools cannot be expected to be larger than a finite cutoff size. However, large schools or groups of animals are required for sustainability and wildlife preser-

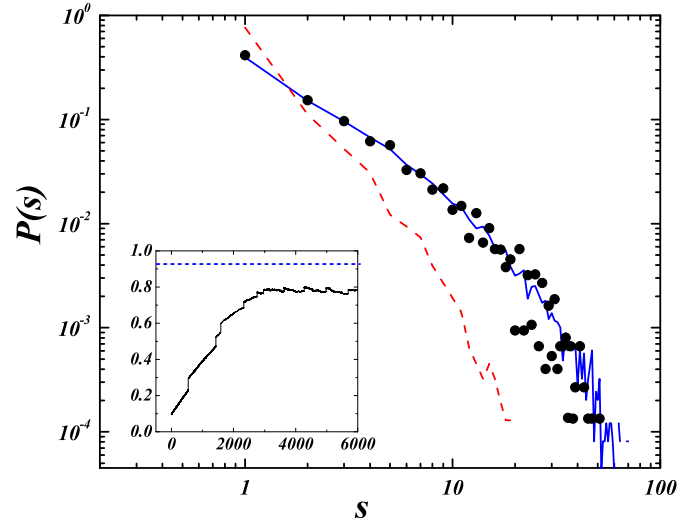


Fig. 5. School size distribution of free-swimming tuna (shaded circles), and of a nonconservative system with $\epsilon = 0.15$ and $\eta N = 409.5$ taken after 2^{15} time steps (solid curve). Also shown is a size distribution resulting from an equivalent SOBP model (dashed curve) having the same value of $q_c = 0.952$ as the nonconservative model. Inset graph reveals the evolution of $q(t)$. Its steady-state value q^* is less than q_c (dashed line), implying that the nonconservative system is sub-critical.

vation as it is believed that group size affects reproductive success of animals, most especially endangered species.

Lastly, it is also interesting to note that for $\eta N \simeq \theta$, the q^* value is highly uncertain to small variations in either η or N . This is the regime describing the abrupt rise from 0 to 1 in figure 4.

4 Recommendations

A key assumption in the model rests upon having the branching parameter defined in eq. (5) sufficiently close to its critical value of 1. With α and β fixed, $\sigma = 1$ is obtained solely by the incorporation of a background activity. This background activity is coupled to the avalanche via a matching condition [eq. (7)] to guarantee that $q = (2\alpha + \beta)^{-1}$ at the steady state. As a modification, one could assume instead that both α and β also change with t , perhaps due to some local feedback mechanism that adjusts the branching probability depending on the history of an agent's activity. Hence in general eq. (6) may be written as

$$\frac{d\sigma}{dt} = \left(2 \frac{\partial \alpha}{\partial t} + \frac{\partial \beta}{\partial t} \right) q + (2\alpha + \beta) \frac{\partial q}{\partial t}.$$

The implementation of the above modification lies in defining the feedback mechanism that gives $\partial \alpha / \partial t$ and $\partial \beta / \partial t$. Lastly, the model can be extended to the case wherein $\{z\} = \{0, 1, 2, \dots, z_{th}, z_{th} + 1\}$ and $z_{th} > 1$. Preliminary research is underway to evaluate the performance of the model with these modifications.

5 Summary and Conclusion

In summary, I have proposed a mean-field sandpile model coupled with a background activity that is characterized by local fluctuations between stable agent states. Even in the presence of violation of the grain-transfer rule, the sandpile can self-organize to a critical state. This result addresses the long-standing issue of whether SOC is possible in nonconservative sandpiles. The model is applied to explaining the truncated school size distribution observed for free-swimming tuna and provides insight into the effects of population depletion on the aggregation capacity of clustering animals. Lastly, some recommendations for extending the model have been rendered.

The author wishes to acknowledge the OVCRD in UP Diliman for Grant No. 050501 DNSE, and the PCASTRD-DOST for funding this research.

References

1. A. Vespignani and S. Zapperi, Phys. Rev. E **57**, (1998) 6345-6362.
2. T. Tsuchiya and M. Katori, Phys. Rev. E **61**, (2000) 1183-1188.
3. S. Zapperi, K.B. Lauritsen, and H.E. Stanley, Phys. Rev. Lett. **75**, (1995) 4071-4074; K.B. Lauritsen, S. Zapperi, and H.E. Stanley, Phys. Rev. E **54**, (1996) 2483-2488.
4. B. Drossel, Phys. Rev. Lett. **89**, (2002) 238701; S.T.R. Pinho and C.P.C. Prado, Braz. J. Phys. **33**, (2003) 476-486; C.J. Boulter and G. Miller, Phys. Rev. E. **68**, (2003) 056108.
5. B. Drossel and F. Schwabl, Phys. Rev. Lett. **69**, (1992) 1629-1632.
6. J.E.S. Socola, G. Grinstein, and C. Jayaprakash, Phys. Rev. E **47**, (1993) 2366-2376.
7. V. Loreto, L. Pietronero, A. Vespignani, and S. Zapperi, Phys. Rev. Lett. **75**, (1995) 465-468.
8. H.E. Stanley, L.A.N. Amaral, P. Gopikrishnan, P.Ch. Ivanov, T.H. Keitt, and V. Plerou, Physica A **281**, (2000) 60-68; T. Gisiger, Biol. Rev. **76**, (2001) 161-209; M. Pascual and F. Guichard, Trends. Ecol. Evol. **20**, (2005) 88-95.
9. J.J. Tyson and J.P. Keener, Phys. D **32**, (1988) 327-361; E. Meron, Phys. Rep. **218**, (1992) 1-66.
10. T.E. Harris, *The Theory of Branching Processes* (Springer-Verlag, Berlin 1963).
11. S.H. Strogatz, *Nonlinear Dynamics and Chaos: With Applications to Physics, Biology, Chemistry, and Engineering* (Perseus Books, Reading MA 1994).
12. R.L. Mendes, A.A. Santos, M.L. Martins, and M.J. Vilela, Physica A **298**, (2001) 471-487.
13. E. Bonabeau, L. Dagorn, and P. Fréon, Proc. Natl. Acad. Sci. USA **96**, (1999) 4472-4477.

